Crystalline Phases of Alkyl-Thiol Monolayers on Liquid Mercury

B. M. Ocko,[1,*] H. Kraack,[2] P. S. Pershan,[3] E. Sloutskin,[2] L. Tamam,[2] and M. Deutsch[2]

[1]*Department of Physics, Brookhaven National Laboratory, Upton, New York 11973, USA*
[2]*Department of Physics, Bar-Ilan University, Ramat-Gan 52900, Israel*
[3]*Department of Physics, Harvard University, Cambridge, Massachusetts 02138, USA*

(Received 7 October 2004; published 12 January 2005)

The structure of octadecanethiol monolayers on liquid Hg surfaces, measured with subangstrom resolution, evolves with increasing coverage from a laterally disordered phase of surface-parallel molecules to ordered rotator phases of surface-normal molecules. For the latter, an abrupt transition is found at 19 Å^2/molecule from a rectangular packing of molecules tilted by 27° in the nearest-neighbor direction to a hexagonal unit cell of untilted molecules. The unit cell of the tilted phase is centered for the chains and noncentered for the headgroups. The thiol headgroups associate in pairs with a single Hg atom, and the bonds form long-range orientational order. The different order of thiols on Au(111) and on Hg highlights the subphase's role in determining the overlayer's structure.

DOI: 10.1103/PhysRevLett.94.017802 PACS numbers: 68.18.Jk, 68.18.Fg

The nature and pathways of charge transfer in single organic molecules, and the processes involved therein, are among the most intensely studied open questions in the field of molecular electronics [1]. The majority of the experimental studies addressing this question employ self-assembled monolayers (SAMs) on solid substrates, most notably alkyl thiols on gold [2,3]. However, recent charge transfer studies between thiol-covered Hg electrodes and solid metals [4,5], semiconductors [6], and liquid Hg [7,8] demonstrate the great advantages of liquid Hg substrates for these studies. These surfaces are atomically smooth, lack long-range order of their own, and have no steps and structural defects. At the same time, their strong chemical bond with the thiol headgroup is preserved. Moreover, unlike solid-supported monolayers, the areal density of molecules in a Hg-supported monolayer, and hence its charge transfer properties, can be easily and continuously varied *in situ* by employing Langmuir trough techniques. Thus, the liquid Hg substrate used in this study is an ideal substrate for growing variable-density, macroscopic-sized, highly perfect SAMs [9], which reflect the monolayer's intrinsic structure rather than that imposed epitaxially by the substrate.

A detailed knowledge of the structure of a SAM is a prerequisite for any study of its charge transport, and other molecular-electronics-oriented properties. Thus, alkyl-thiol monolayers on a solid Au(111) substrate were extensively studied [10,11]. They exhibit a variety of different phases, e.g., a striped phase of lying-down molecules and a $c(4 \times 2)$-ordered tilted phase of standing-up molecules. For all phases the epitaxy to the crystalline Au dominated the structure of the monolayer. By contrast, only two high-resolution structural studies of Hg-supported alkyl thiols, by x rays [12], and by tip microscopy [13], have been published to date. Both addressed only high surface density films and failed to detect any lateral structure in the films.

We present here a subangstrom-resolution x-ray study of the structure of an octadecanethiol (C18S) monolayer on a liquid Hg surface, and its coverage dependence. The results are contrasted with those found for SAMs on Au and Langmuir films on water [14]. The comparison highlights the important role of the substrate-molecule interaction in the determination of the film's structure.

The surface pressure (π) molecular area (A) isotherm of C18S, shown in the inset to Fig. 1(a) (open circles and interpolating line), was measured by the stepwise deposition of a solution of C18S in chloroform. The nominal A is the trough area divided by the number of deposited molecules. For $A \geq 120$ Å^2/molecule, the isotherm is reason-

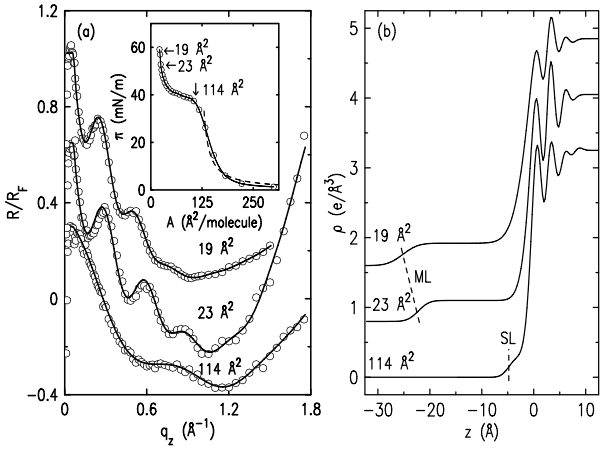

FIG. 1. (a) Fresnel-normalized x-ray reflectivity (points), and "box-model" fits (lines) for C18S on Hg at the indicated coverages A, and $T = 25\,^\circ$C. $q_z = (4\pi/\lambda)\sin(\alpha)$, where $\lambda = 1.56$ Å is the wavelength, and α is the grazing incidence angle, of the x rays used. Inset: the measured isotherm (points). The arrows mark the A values where reflectivities were measured. (b) The fit-determined surface-normal electron density profiles. The oscillations at $z > 0$ are due to the surface-induced layering in the Hg. The plateaus at $z < 0$ are the organic layers. ML and SL are the monolayer of standing-up molecules and the single-layer of lying-down molecules, respectively.

ably well fitted by the Volmer equation of a 2D "ideal" gas law (dashed line), $\pi(A - A_1) = k_B T$. The fitted exclusion area, due to the finite molecular size, $A_1 = (118 \pm 8)$ Å^2/molecule, agrees closely with the 121 Å^2/molecule calculated from the known molecular width (4.8 Å) and length (25.2 Å). As shown for stearic acid on Hg [15,16], this indicates that at $A \approx 120$ Å^2/molecule the film is a closely packed monolayer of lying-down molecules. Similar isotherms for other-length alkyl thiols, CnS, with $n = 12$, 14, and 22, yield a linear $A_1 = (6.04 \pm 0.3) \times n + (10 \pm 6)$ Å^2/molecule [17]. The coincidence of the slope, ~6 Å^2/molecule per carbon, with the area, 1.27×4.8 Å^2, of a lying-down CH_2 group, further supports the conclusions above identifying the $A \geq 120$ Å^2/molecule phase. Similarly, the single plateau observed for $35 \leq A \leq 120$ Å^2/molecule and the steep rise in the isotherm at low $A \leq 35$ Å^2/molecule hint at a coexistence region between lying-down and standing-up molecules, and condensed phases of standing-up molecules, respectively, as found for fatty acids [15,16]. Since definite structural conclusions cannot be drawn from the isotherm alone, we now proceed to discuss our x-ray measurements.

Specular x-ray reflectivity (XR) probes the surface-normal electron density profile. Figure 1(a) shows a set of measured XRs (open circles), normalized to the Fresnel reflectivity, R_F, of an ideally flat and smooth surface, along with their box-model [15,16] fits (line), all providing excellent agreement with the measured points. The surface-normal electron density profiles derived from these box-model fits are shown in Fig. 1(b). The rise in all R/R_F curves at $q_z > 1.5$ Å^{-1} is due to surface-induced layering in the Hg subphase [18]. The Kiessig fringe period in R/R_F is observed to decrease with decreasing A. At $A = 19$ Å^2/molecule, the period, $\Delta q_z = 0.25$ Å^{-1}, yields a layer thickness of $d = 2\pi/\Delta q_z = 25$ Å, close to the length of a fully extended molecule, 25.2 Å. The box-model fit (solid line) yields (25.2 ± 0.4) Å. We conclude therefore that at this coverage the film is a monolayer of surface-normal aligned molecules. At $A = 114$ Å^2/molecule, the fit reveals a uniform film of thickness of $d = 4.8$ Å and an electron density $\rho = 0.30\ e/$Å^3. These values are in excellent agreement with the interchain distance and the electron density of close-packed alkyl chains [19]. This, and the Volmer exclusion area, strongly supports the conclusion that for $A \approx 114$ Å^2/molecule the film is a dense single layer of surface-parallel molecules. The high surface tension of Hg, $\gamma \approx 500$ mN/m, yields a very low surface roughness, ~1 Å, which permits accurate thickness determinations of these very thin films. At 23 Å^2/molecule the fit yields $d = 22.2$ Å. This, and the 25.2 Å length of a fully extended molecule, suggests at this coverage a monolayer of standing-up molecules, tilted by $(28 \pm 3)°$ from the surface normal. In the plateau region of the isotherm, between 30 and 90 Å^2/molecule, the XR curves (not shown) can be fitted only by a model assuming a coexistence of the (tilted) standing-up and the lying-down phases. At a coverage of $A = 19$ Å^2/molecule, a partial untilted standing-up phase, coexisting with a tilted phase, could be produced directly at 25 °C. Cooling to 10 °C yielded a uniform untilted phase, which remained stable upon subsequent heating to 25 °C.

The in-plane order was probed by grazing incidence diffraction (GID) and Bragg rod (BR) measurements at the GID peak positions. BR scans yield information on the thickness of the laterally ordered phases, on the direction and magnitude of the chain tilt, and on the formation of a mercury thiolate in the headgroup. For the lying-down phases no GID peaks were observed indicating that these phases are disordered laterally. This is in contrast with the lying-down phases of fatty acid monolayers on Hg, which were found to be ordered laterally [15,16]. However, the standing-up phases of alkyl thiols on Hg do exhibit well ordered phases which we now discuss.

A GID scan at $A = 23$ Å^2/molecule is shown in Fig. 2. In contrast with previous measurements [12], which did not show any GID peaks [20], eight distinct, resolution limited, diffraction peaks are observed here between $0.5 \leq q_{\|} \leq 3.0$ Å^{-1}. These peaks can be indexed to within ± 0.002 Å^{-1} in a *noncentered* rectangular unit cell of dimensions $\mathbf{a} = 5.51$ Å and $\mathbf{b} = 8.42$ Å, with two molecules per cell. The presence of the odd-$(h + k)$ peaks is the unambiguous signature of a noncentered cell. SAMs of alkyl thiols on a solid Au(111) substrate [11] also show a noncentered unit cell, often referred to by the larger $c(4 \times 2)$ supercell. Noncentered cells have not been hitherto reported for monolayers of any chain molecule on Hg [15,16] or on water [14], although such cells were obtained

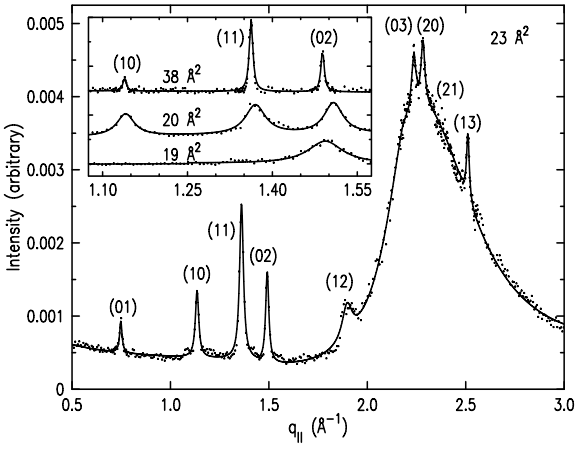

FIG. 2. GID pattern for C18S at 23 Å^2/molecule. Here $\alpha < \alpha_c$, the critical incidence angle for total external reflection, we scan the angle from the reflection plane, 2θ, and $q_{\|} \cong (4\pi/\lambda) \times \sin(2\theta/2)$. The sharp diffraction peaks, originating in the structure of the monolayer, can be indexed in a (noncentered) rectangular unit cell. The broad peak at $q_{\|} \approx 2.3$ Å^{-1} is due to the liquid structure factor of the Hg. The inset shows the evolution of the low-order peaks with coverage.

for subphases of aqueous solutions of some (though not all) divalent metal ions [21].

The contour plots and BRs, Fig. 3, for the (10), (11), and (02) GID peaks of Fig. 2 reveal a richer and more intriguing structure than the noncentered unit cell concluded from the GID alone. Two types of BRs are observed: long [e.g., (10) in Fig. 3(d)] and short [e.g., (02)] in the q_z direction. A BR's half length at half maximum, Δq_z^{BR}, yields the thickness $d^{\mathrm{BR}} = \pi/\Delta q_z^{\mathrm{BR}}$ of the layer which gives rise to the BR. For our two types, $\Delta q_z^{\mathrm{BR}} \approx 0.7$ and 0.15 Å^{-1} yield $d^{\mathrm{BR}} \approx 4.5$ and 23 Å for (10) and (02), respectively. Detailed modeling [17], shown in solid lines in Figs. 3(a)–3(c), fully concurs with these results. The thin and thick layers can be identified, therefore, with the molecules' headgroups and aliphatic tails, respectively. The (11) BR in Figs. 3(b) and 3(d) is a superposition of both a short BR and a long BR, indicating contributions from both the headgroups and the tails. A careful examination of all BRs reveals that the odd-$(h + k)$ ones comprise only long BRs, while only the even-$(h + k)$ ones include short BR contributions (although they may also include long BR contributions). Thus, the odd-$(h + k)$ GID peaks originate exclusively in the headgroups' layer, while the tails' layer contributes only to even-$(h + k)$ GID peaks. This leads to the conclusion that while the headgroups order in a *noncentered* rectangular cell, the tails order in a *centered* rectangular cell [22].

We discuss first the tails' centered unit cell, based on the short BR components of the two lowest-order peaks originating in this layer, (11) and (02). Their $(q_\parallel, q_z)$ peak coordinates, (1.36,0.6) and (1.49, 0) Å^{-1}, and the detailed modeling [17], indicate that the tails in this layer tilt from the surface normal by $(27 \pm 1)°$ in the nearest-neighbor (NN) direction. This is the tilt required for a 2-carbon shift between adjacent chains, which moves the "tooth" of one zigzag chain to the next "depression" in an adjacent zigzag chain. In the plane perpendicular to the tails this yields a unit cell $5.51\cos(27)° \times 8.42 = 4.91 \times 8.42$ Å^2. The resultant x-ray-derived area per molecules in the plane perpendicular to the molecular long axis, $A_\perp = 20.66$ Å^2/tail, is typical of a rotator phase and not of a herringbone-ordered crystalline phase which has a molecular area 18.5–19.0 Å^2/molecule [19]. Moreover, the ratio $8.42/4.91 \approx \sqrt{3}$ proves that the tails pack hexagonally in this plane. These results identify the structure of the tails' layer as the L_{2d} phase of fatty acid monolayers on water [14].

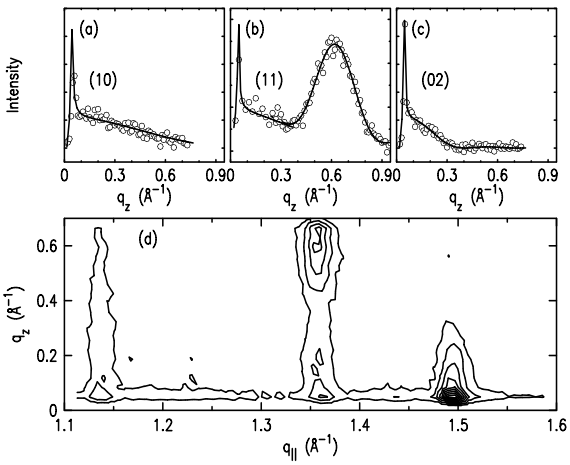

FIG. 3. (a)–(c) Measured (circles) and model fitted (lines) Bragg rods for the indicated GID peaks. The sharp surface-enhancement peaks near the origin ("Vineyard" peaks) are due to interference between incident and diffracted rays at the critical angle. For Bragg rods peaking at $q_z = 0$ Å^{-1} only the positive half of the peak is observed. (d) Equal-intensity contour plot of these peaks.

The headgroups' noncentered order can be traced to the chemistry of the thiol moiety. As the short and long BRs originate, respectively, in the tails and headgroups of the alkyl thiols, the ratio of their contributions (integrated over q_z) to the intensity of the low-q_z GID peaks in Fig. 2 is related to the ratio R_e of the number of scattering electrons in these two parts of the molecule. The 1:1.5 ~ 1:3 BR intensity ratio found implies an R_e significantly larger than the 17/145 expected from the SH : $CH_3(CH_2)_{17}$ composition of the molecule. This argues against the two-molecule S-S hybridization (disulfide), suggested for alkyl thiols on Au [11], as the origin of the noncentered headgroups' cell, since this does not significantly change R_e. Rather, the high intensity ratio suggests the incorporation of a single Hg atom per two thiol molecules into the headgroups' layer to form a covalent S-Hg-S bond. This conclusion is supported by the 1:2 Hg:thiol stoichiometry found in bulk Hg thiolates [7], where the strong covalent S-Hg-S bond is found to involve a transfer of one electron per thiol with the corresponding loss of the terminal hydrogen. In contrast, on Au(111), only a partial transfer, ~0.3 electrons per thiol, is found [23]. We also note that the equal $q_\parallel$ widths of the odd- and even-order GID peaks in Fig. 2 imply not only equal crystalline coherence lengths for both the tails' and the headgroups' layers, but also a long-range orientational order for the S-Hg-S bonds [24].

The positions of the GID peaks remain nearly the same down to $A = 20$ Å^2/molecule (Fig. 2 inset), implying no change in the crystalline order in either the tails or the headgroups, except for a reduction in the crystalline coherence length, ξ, reflected in a broadening of the peaks. At $A = 19$ Å^2/molecule (after cooling and reheating) the GID pattern changes abruptly to a single peak at $q_\parallel = 1.50$ Å^{-1}, with a short BR which peaks at $q_z = 0$ Å^{-1}. These values indicate a hexagonal LS-like rotator phase of surface-normal molecules [14], with a lattice constant of 4.84 Å and $A_\perp = 20.35$ Å^2/molecule. The single GID peak's width, 0.074 Å^{-1}, yields $\xi \approx 90$ Å only, as compared to $\xi > 1000$ Å obtained from the resolution limited peaks at $A = 38$ Å^2/molecule. This reduction in ξ, reflecting a packing frustration, may originate in the S-Hg-S bond

orientation disorder arising from the absence of a unique preferred direction for the bond in the hexagonal phase. A similar explanation accounted for the reduction in ξ upon lateral polymerization in monolayers of octadecyltrichloromethylsilane on silicon [25].

The discontinuous transition from a 27°-tilted L_{2d} phase to a nontilted LS one appears to be first order, with a coexistence between the two phases for $19 \leq A \leq 23$ Å^2/molecule. Although the tilted phase exhibits a 1.6% decrease in $A_\perp$ as A decreases from 38 to 20 Å^2/molecule, the tilt remains virtually unchanged. In contrast, the L_2-to-LS transition in fatty acid monolayers on water exhibits a continuous decrease in the tilt with A. The relative intensities of the odd- and even-$(h + k)$ GID peaks remain roughly constant in the coexistence region. This suggests that no change occurs in the structure of the S-Hg-S bond orientational order in the L_{2d} phase as the transition is approached, except for the change in ξ mentioned above.

C18S on Au(111) is perhaps the most extensively studied SAM [2]. Its full-coverage phase has a structure commensurate with that of Au(111), with $A_\perp = 18.7$ Å^2/molecule, very close to the $A_\perp = 18.4$ Å^2/molecule of a herringbone packing, and a molecular tilt of 30° in a direction 8°–10° away from the next nearest-neighbor direction [2,11]. Stearic acid on mercury, with its larger headgroup, has a molecular area of $A_\perp = 19.6$ Å^2/molecule and a tilt decreasing continuously with A [15,16]. These should be contrasted with C18S on Hg, which exhibits rotator phases only, with $A_\perp = 20.35$–20.66 Å^2/molecule, a constant 27° molecular tilt in the NN direction, and an abrupt rectangular-to-hexagonal, tilted-to-untilted transition. These structural differences originate most likely in the different nature of, and the headgroups' interaction with, the subphase. The liquid Hg's lack of long-range order, and the high mobility of its atoms, eliminate the epitaxial constraints present for Au(111), in spite of the strong S-Hg-S bond. At the same time, this very bond may produce constraints on the tilt's magnitude, direction, and stability, especially compared with stearic acid which does not bind as strongly. Moreover, the length and the orientation preferred by the bond for creating long-range orientational order may dictate a rotator, rather than a herringbone, packing. Studies, now in progress, of the variation of the structure found here with the alkyl thiol's chain length and the temperature should provide new insights into the factors dominating the monolayer's structure. The present results, especially the formation of the S-Hg-S bond and the lower chain packing density than that on Au, may provide better understanding of, and allow new ways of tuning, the charge transfer properties across the thiol monolayer and the thiol-Hg junction.

Support to M. D. by the U.S.–Israel Binational Science Foundation, Jerusalem, and to P. S. P. by the U.S. DOE (Grant No. DE-FG02-88-ER45379) is gratefully acknowledged. BNL is supported by U.S. DOE Contract No. DE-AC02-98CH10886.

*Electronic address: ocko@bnl.gov

[1] B. A. Mantooth and P. S. Weiss, Proc. IEEE **91**, 1785 (2003); *Molecular Electronics*, edited by J. Jortner and M. Ratner (Blackwell, Oxford, 1997)
[2] F. Schreiber, Prog. Surf. Sci. **65**, 151 (2000); J. Phys. Condens. Matter **16**, R881 (2004).
[3] A. Ulman, *An Introduction to Ultrathin Organic Films* (Academic Press, Boston, 1991).
[4] M. A. Rampi and G. M. Whitesides, Chem. Phys. **281**, 373 (2002).
[5] M. Galperin, A. Nitzan, S. Sek, and M. Majda, J. Electroanal. Chem. **550**, 337 (2003).
[6] Y. Selzer, A. Salomon, and D. Cahen, J. Am. Chem. Soc. **124**, 2886 (2002).
[7] K. Slowinski *et al.*, J. Am. Chem. Soc. **119**, 11 910 (1997).
[8] K. Slowinski and M. Majda, J. Electroanal. Chem. **491**, 139 (2000).
[9] J. Michl and T. F. Magnera, Proc. Natl. Acad. Sci. U.S.A. **99**, 4788 (2002).
[10] L. Strong and G. Whitesides, Langmuir **4**, 546 (1988); C. E. D. Chidsey and D. N. Loiacono, *ibid.* **6**, 682 (1990); G. E. Poirier, *ibid.* **15**, 1167 (1999); N. Camillone *et al.*, J. Chem. Phys. **101**, 11 031 (1994).
[11] P. Fenter, A. Eberhardt, and P. Eisenberger, Science **266**, 1216 (1994).
[12] O. M. Magnussen *et al.*, Nature (London) **384**, 250 (1996).
[13] C. Bruckner-Lea *et al.*, Langmuir **9**, 3612 (1993).
[14] V. M. Kaganer, P. Dutta, and H. Möhwald, Rev. Mod. Phys. **71**, 779 (1999).
[15] H. Kraack *et al.*, Science **298**, 1404 (2002).
[16] H. Kraack *et al.*, Langmuir **20**, 5375 (2004); **20**, 5386 (2004).
[17] H. Kraack *et al.* (to be published).
[18] O. M. Magnussen *et al.*, Phys. Rev. Lett. **74**, 4444 (1995); E. DiMasi *et al.*, Phys. Rev. B **58**, 13 419 (1998).
[19] D. M. Small, *The Physical Chemistry of Lipids* (Plenum Press, New York, 1988).
[20] The absence of in-plane peaks in Ref. [12] is probably due to beam damage. The GID peaks vanished upon exposures of 0.1–1 photons/molecule. Thus, the trough was translated periodically to illuminate a fresh area each time.
[21] F. Leveiller *et al.*, Science **252**, 1532 (1991); I. Kuzmenko *et al.*, Chem. Rev. **101**, 1659 (2001); J. Kmetko *et al.*, J. Phys. Chem. B **105**, 10 818 (2001).
[22] An alternative description by an oblique lattice of tails, with a 1×2 superlattice of headgroups, is also possible.
[23] P. Krysinski, R. V. Chamberlain, and M. Majda, Langmuir **10**, 4286 (1994).
[24] The fast beam damage did not allow collecting GID data with reliable intensity ratios of the GID peaks to support a full crystallographic refinement.
[25] R. Maoz, J. Sagiv, D. Degenhardt, H. Möhwald, and P. Quint, Supramol. Sci. **2**, 9 (1995).